Journal of the Geological Society

An Oldest Dryas glacier expansion in the Pelister Mountain (Former Yugoslavian Republic of Macedonia) according to 10Be cosmogenic dating

--Manuscript Draft--

Manuscript Number:	jgs2017-038R1
Article Type:	Research article
Full Title:	An Oldest Dryas glacier expansion in the Pelister Mountain (Former Yugoslavian Republic of Macedonia) according to 10Be cosmogenic dating
Short Title:	Cosmogenic age of an Oldest Dryas glacial advance
Corresponding Author:	Adriano Ribolini, Ph.D Universita degli Studi di Pisa Pisa, ITALY
Corresponding Author E-Mail:	ribolini@dst.unipi.it
Other Authors:	Monica Bini
	Ilaria Isola
	Matteo Spagnolo
	Giovanni Zanchetta
	Ramón Pellitero
	Silke Mechernich
	Raphael Gromig
	Tibor Dunai
	Bernd Wagner
	Ivica Milevski
Manuscript Classifications:	Dating (radiometric, absolute, etc); Geomorphology
Additional Information:	
Question	**Response**
Are there any conflicting interests, financial or otherwise?	No
Samples used for data or illustrations in this article have been collected in a responsible manner	Confirmed
Response to Reviewers:	Dear Editor, we submit a revised version of the manuscript "An Oldest Dryas glacier expansion in the Pelister mountain (Former Yugoslavian Republic of Macedonia) according to 10Be cosmogenic dating" for consideration by the Journal of the Geological Society. The manuscript has been revised accordingly to the comments of the reviewers. We have uploaded a "reply to reviewers" letter to list the requested changes, and those that we cannot do providing the reasons. In particular we have better detailed the laboratory procedures (reporting chemical analytical results in the supplementary material and an extended description in the Method section). Moreover, the method used for exposure age calculation is now clearer (adding the new Table 2), reporting also the adopted scaling system for spallation and the possible results coming from other models. The procedure to calculate the ELA is now better detailed by adding several lines in the Methods section. The sources of the information necessary to automatically

	reconstruct the palaeo-glacier have been better acknowledged. All the comments by the Editor have been considered We hope that now the paper may be considered for the publication by the Journal of the Geological Society. Best regards Adriano Ribolini

AN OLDEST DRYAS GLACIER EXPANSION IN THE PELISTER MOUNTAIN (FORMER YUGOSLAVIAN REPUBLIC OF MACEDONIA) ACCORDING TO ^{10}BE COSMOGENIC DATING

ADRIANO RIBOLINI[1*], MONICA BINI[1], ILARIA ISOLA[2], MATTEO SPAGNOLO[3], GIOVANNI ZANCHETTA[1], RAMÓN PELLITERO[3], SILKE MECHERNICH [4], RAPHAEL GROMIG[4], TIBOR· DUNAI[4], BERND WAGNER[4] & IVICA MILEVSKI[5]

[1] Department of Earth Sciences, University of Pisa, Italy
[2] Istituto Nazionale di Geofisica e Vulcanologia, Pisa, Italy
[3] School of Geosciences, University of Aberdeen, Scotland
[4] Institute of Geology and Mineralogy, University of Cologne, Germany
[5] Faculty of Natural Sciences and Mathematics, University of Skopje, Macedonia
* correspondence: ribolini@dst.unipi.it

Abstract

We provide a geomorphological analysis of a glacial valley in the Pelister mountain, in Macedonia. Three boulders from a frontal moraine were dated with cosmogenic nuclide isotope ^{10}Be. Results demonstrate that the boulders have been exposed since 15.24 ± 0.85 ka. This age constrains the formation of the frontal moraine to the Oldest Dryas cold event. This age fits with that of the other glacier deposits dated to the Older Dryas in the Alps, Balkans, Carpathians and Turkey mountains. The Pelister palaeo glacier has been reconstructed and its equilibrium line altitude extracted, returning of a value of 2,250 m asl. This is in good agreement with the equilibrium line altitudes of most other reconstructed glaciers of the same age in the circum-Mediterranean mountains, demonstrating a comparable response to the Oldest Dryas event. Other palaeoenvironmental records near the Pelister mountain indicate that the Older Dryas was here characterized by a cold and remarkably-dry event. The temporal relationship between Older Dryas glacier advances in the Balkan region and recorded changes in the Atlantic thermohaline circulation during the Laurentide Ice Sheet massive ice discharge (H1 event), confirms the strong climatic link between the pan Mediterranean regions and the North Atlantic Ocean.

Supplementary material: geochemical laboratory results are available at: http://geolsoc.figshare.com

In the last decades, the increased interest on the size and geometry of palaeo glaciers in the pan-Mediterranean region and their climatic significance has stimulated a number of new studies on many of its mountain ranges (Hughes *et al.* 2006a; Hughes & Woodward 2008; 2017 and reference therein). The chronological information included in some of these data has been used to interpret glacier dynamics and, when integrated with other terrestrial and marine climate proxies, to derive palaeoevironmental conditions (Federici *et al.* 2017; Palacios *et al.* 2017). In particular, palaeoglaciological reconstructions can be used to infer the climate of the past, based on the paradigm that glaciers respond to changes in air temperature and precipitation by adjusting their mass balance with a consequent advance/retreat of the glacier's front (Oerlemans 2005).

The climate of the Mediterranean mountains is influenced by atmospheric perturbations originated off the North Atlantic, along with southward outbreaks of the polar front and of the Siberian high pressure (Lionello *et al.* 2006; Florinet & Schlüchter 2000; Kuhlemann *et al.* 2008). Moreover, zones of cyclogenesis can be generated in the central Mediterranean area (Gulf of Lions and Genova) as well as in the subtropical high-pressure zone. How these various components interplayed in the past remains an unresolved and discussed question in palaeoclimatology (Kuhlemann *et al.* 2008). Within this context, the behavior of Mediterranean mountain glaciers across the last glacial cycle may help to unravel the effect of the various climatic components that affected the Mediterranean atmospheric circulations during this time.

The chronological data collected so far indicate that, following the Last Glacial Maximum (~23 ka, LGM hereafter, Hughes & Gibbard 2015), the Mediterranean mountain glaciers recorded at least two Late-glacial (~23-10 ka) advances, approximately at 16-15 ka and 13-11 ka (Giraudi & Frezzotti 1997; Ivy-Ochs *et al.* 2006; Federici *et al.* 2008; Hughes & Woodward 2008; Akçar *et al.* 2014; Hughes & Gibbard 2015; Federici *et al.* 2017; Palacios *et al.* 2016). These two advances match with the cold periods known as GS-2a and GS-1 stadials recognized in the oxygen isotope record of Greenland cores (Björk *et al.* 1998; Rasmussen *et al.* 2006), and with the Oldest and Younger Dryas in many other studies (Clark *et al.* 2012; Palacios *et al.* 2017 and reference therein).

Despite the relative large number of recent publications, the distribution of chronologically-constrained glacier advances is spatially discontinuous, with some mountain ranges still completely or partially unstudied. For example, in the Dinaric Alps and Greek mountains, the LGM and older glacial cycles are well documented (Hughes *et al.* 2003; 2006a; 2010), whereas Late-glacial advances are less documented and rarely dated, with the exception

of the mountains of Kosovo and Montenegro (Kuhlemann *et al.* 2008; Hughes *et al.* 2011). Even worse is the situation of the mountainous regions within the Former Yugoslavian Republic of Macedonia (from now on referred to as Macedonia). Here, despite evidence of multiple glacier advances (Menković *et al.* 2004; Ribolini *et al.* 2011; Milevsky 2015), no chronological constraints have ever been obtained, thus putting this region completely outside of the palimpsest of cold climate events of the Mediterranean.

The aim of this work is to illustrate the glacial geomorphology and chronology of a frontal moraine in the Pelister mountain range, SW Macedonia (Fig. 1). The ages, obtained by cosmogenic ^{10}Be dating of the glacial deposit, and the equilibrium line altitude (ELA) of the reconstructed glacier that deposited it, are then discussed in the context of other glacier advances of similar age across the Mediterranean, as well as in relation to other palaeoenvironmental records.

Setting

The Pelister mountain range (Fig. 1) is characterized by a number of summits exceeding an elevation of 2,500 m asl, with the Pelister peak being the highest at 2,601 m asl.

Similar to the other mountain ranges belonging to the West Macedonian Zone (Arsovski 1997), the Pelister's has a NE-SW main axis strike. Since the Late Caenozoic, the area experienced differential movements along normal, oblique and strike slip faults that led to the formation of horst and graben systems roughly aligned to the NE-SW direction. Some of these grabens are now filled by lakes, such as the Ohrid and Prespa lakes (Burchfiel *et al.* 2004; Hoffmann 2013; Milevski 2015). From the main watershed, the Pelister mountain flanks steeply descend towards the Lake Prespa and Bitola plain, to the W and E respectively. Three valleys drain the eastern flank, all joining a main SW-NE oriented river that runs along the mountain's foot, and which enters the Bitola plain. One of these valleys, the Veternica Valley, hosts a typical glacial cirque lake, the Golemo Ezero (Fig. 2), in its uppermost part. The lake is located at 2,222 m asl, in proximity to the main watershed, between the Veternica (2,420 m asl) and Mrazarnik (2,236 m asl) peaks. It is 17 m deep and is dammed by a moraine, which is the focus of the chronological work and palaeoglacier reconstruction presented here.

The bedrock of the Pelister mountain range is mainly composed of an Ordovician alkaline-granites and granodiorites, frequently embedded within Paleozoic shales, and quartz- and quartz-sericite schists. Locally, amphibolites and amphibolite-schists crop out.

The geomorphology of the region includes cirques and thick glacial and fluvio-glacial deposits, along with extensive periglacial landforms such as block streams, block fields, solifluction lobes and ploughing blocks (Stojadinović 1970; Kolčakovski 1996; Andonovski & Milevski 2001).

As it was not possible to retrieve any local meteorological data, climate information was sourced from a global dataset obtained by interpolating weather stations at a resolution of 30 arc seconds (http://www.worldclim.org) (Hijmans *et al*. 2005). From this, it appears that the top of the Vertnica Valley is presently characterized by total annual precipitation of 980 mm, with November and August being the wettest (110 mm) and the driest (53 mm) months respectively. The mean annual temperature is 2.7 °C, with January and July being the coldest (-5.8 °C) and warmest (11.5 °C) months respectively.

Methods

The Veternica Valley was surveyed during two field campaigns in 2013 and 2014. The survey led to detailed geomorphological mapping undertaken on topographic maps at 1:25,000 scale. The mapping was later implemented by the analysis of satellite imagines (Quick Bird imagery: QB02 sensor and Pan_MS1 band, 60 cm spatial resolution). Sampling and dating were focused on the frontal moraine that dams the Golemo Ezero Lake. The moraine is matrix-supported and characterized by a large number of boulders resting on its crest. The top surface of three of these boulders was sampled for the purpose of obtaining an exposure age through the measurement of the ^{10}Be cosmogenic isotope concentration. The sampled boulders stand 0.5 to 1 meter above the surrounding moraine's crest and are characterized by a quartz-rich crystalline and metamorphic lithology, i.e. quartz-rich schist. Each sample was collected from a flat (though not necessarily horizontal) surface as far away as possible from the boulder's edges. Only the first 3-4 cm of rock from the surface of the boulder were collected. The angle to the horizon was measured at 30-degree intervals, as well as the strike and dip of the sampled surface in order to calculate topographic and self-shielding (Dunne *et al*. 1999).

Quartz was obtained from each sample using magnetic separation to isolate iron-bearing minerals, froth flotation to separate feldspars and micas, and density separation to remove heavy minerals. The quartz was finished with hydrofluoric and nitric acid leaches and purity checked with Inductively Coupled Plasma Optical Emission Spectroscopy (ICP-OES) analysis. This purified quartz was spiked with approximately 0.250 mg of Be in a carrier solution prepared from beryl and dissolved in hydrofluoric and nitric acids. After

volume reduction, fluorides were decomposed in sulfuric acid and the resulting solids were converted to chlorides and added to a pH>14 sodium hydroxide solution to remove residual iron, titanium, calcium, and magnesium. Beryllium was precipitated out of this solution, taken up with oxalic acid, and purified on cation columns. Purified beryllium was oxidized in a propane flame, mixed with niobium powder, and packed into stainless steel cathodes for the AMS measurement at PRIME Lab, Purdue University, using standards described by Nishiizumi *et al.* (2007).

Exposure ages were calculated adopting the North-East North American production rate and using LM as time-dependent adaptation scaling scheme (Balco *et al.* 2009). The calculations were undertaken with the online CRONUS-Earth tool (http://hess.ess.washington.edu/math/) version 2.2. A rock density of 2.7 g/cm^3 was considered in the age calculation.

Limited features of weathering (i.e. grooves, cavities, micro-relief) were visible on the surface of sampled boulders, indicating a negligible erosion. Therefore, and because a robust, independent control on the erosion rate could not be obtained, the ages were not corrected for this factor. Analogously, information about boulder snow cover today as well as during the Late-glacial are lacking. Therefore, ages were not corrected for this factor either. By not accounting for erosion and snow cover, the ages discussed in this paper are likely to be some hundred years younger than the actual deposition of the moraine.

Tectonic uplift could cause a production rate lower than expected because the Pelister mountain experienced high vertical movement (up to 4-5 mm/yr) in the Late Quaternary (Lilienberg, 1968). Given the exposure ages, this effect may account for up to ~50-70 meters increase in elevation since the calculated ages. This would have affected the calculated ages by no more than 450 hundred years. Glacial isostatic adjustment can be ruled out for the studied area due to the limited thickness of the palaeoglacier. Accordingly, no corrections were applied for changes in elevation of the sampled boulders.

A GIS approach, based on the numerical technique of Benn & Hulton (2010), has been used to semi-automatically reconstruct the thickness and extent of the former cirque glacier that deposited the sampled moraine (Pellitero *et al.* 2016). The approach is based on a user given shear stress, which by default is set to 100 kilopascals (kpa). In this case a shear stress of 50 kpa has been used in the lower portion of the reconstructed glacier in order to match the ice level suggested by the front-lateral moraine, and a default 100 kpa for the rest of the glacier. Further GIS tools (Pellitero *et al.* 2015) have been adopted to automatically derive the Equilibrium Line Altitude (ELA) value of the reconstructed glacier,

by applying the classic Area Altitude Balance Ratio (AABR) method (Osmatson 2005), with a ratio value of 1.6, same as the average obtained on present-day glaciers in other parts of the Mediterranean mountains (Rea, 2009). The same approach was used to reconstruct the extent of, and calculate the ELAs of, other Mediterranean range palaeo-glaciers, coeval of the glacier that deposited the sampled moraine. Mapped frontal moraines which had been dated to the Oldest Dryas (see location and references in Fig. 5) were used to reconstruct the 3D surface of the glaciers that deposited them. Glacier reconstruction was made using the GIS tool mentioned above (Pellitero et al. 2016) with a standard 100 kilopascals shear stress, and the ASTER DEM as the bedrock DEM, with the exception of the glacial landsystems located in Spain and Italy, for which a better quality DEM was available. The resulting 3D surface was checked with the glacial geomorphology, so the resulting glacier surface properly adapted to the landforms (cirques, frontal and lateral moraines) that evidenced a constraint on its extension. The 3D surface of these palaeo-glaciers were then used to derive their ELA, calculated using the GIS tool described in Pellitero et al. (2015). As done for the Pelister ELA calculation, an Accumulation Area Balance Ratio of 1.6 was used in all pan-Mediterranean ELA reconstructions, following Rea (2009).

Results

Glacial and periglacial evidences

The head of the Veternica Valley is a classic glacial cirque (Fig. 2), with well evident lateral spurs and a steep rock headwall. A minor, relatively smoothed depression along the eastern watershed, 30-40 m above the cirque/valley floor, suggests the presence of a glacial transfluence into the adjacent valley, most likely during the LGM. The cirque floor is at an elevation of approximately 2,200 m asl. Between this elevation and 1,900 m asl, the Veternica Valley is occupied by glacial deposits and interspersed bedrock outcrops (Fig. 2). The deposits are made of massive diamicton supported by a coarse sandy-gravel matrix with frequent decimetric clasts. Numerous metric and plurimetric boulders are standing on the deposit’s surface. The dominant lithologies of the clastic fraction are prevalently quartz- schistose and more rarely granitic.

Locally, moraine ridges can be identified within the glacial deposits (Fig. 3a, b, c). The lowermost frontal moraine is composed of two long lateral ridges converging at about

2,060 m asl. (Fig. 2, 3a and 3b). Right upvalley, a set of ridges delineates two portions of the same, indented, moraine at a similar altitude (2,110-2,120 m asl), separated by the current river channel (Fig. 2, 3a and 3b). Further upvalley, the frontal moraine damming the Golemo Ezero Lake is the most prominent of all the moraines in the valley (Fig. 2 and 3c). It stands 25-30 m above the cirque floor and reaches a maximum elevation of 2,230 m at its eastern end, where it progressively becomes buried under scree deposits. Numerous granite and quartz-schist boulders stand on the moraine crest. Another lateral-frontal moraine system is evident further to the East, close to the cirque wall (Fig. 2 and 3c). This small moraine system partly overlaps onto the lateral flank of the large frontal moraine damming the lake.

Many protalus ramparts are present in the slope deposits on the Valley's western flank and at the base of the eastern side of the cirque wall (Fig. 2 and 3d). The rampart crests are partly coalescent and exhibit a close upvalley concavity. Extended block fields and sheets cover the topmost part of the Valley's slope (Fig. 2).

Chronology

Sampling was restricted to the 3 largest blocks residing on the moraine crest (Fig. 4a, b). The field and laboratories values entered in the age calculator are reported in the Tab 1. The dated boulders from the Golemo Ezero moraine returned overlapping ages of 15.03 ± 0.85 ka, 15.56± 0.85 ka and 15.14 ± 0.86 ka (Tab. 2a), thus demonstrating a considerable consistency. In particular, a constant production rate model and the scaling system for spallation of Lal (1991) and Stone (2000) were chosen. The alternative adoption of time-varying production models would have returned ages that are only a few hundred years younger (Tab. 2b).

The mean age of 15.24 ± 0.85 ka is fully consistent with the Late-glacial stadial known as the Oldest Dryas (Björk *et al.* 1998; Rasmussen *et al.* 2006). Given the good reproducibility of the data, the possibilities that the ages are from boulders that were exhumed from moraine fine matrix (minimum age) or boulders exposed prior to be deposited in the fontal moraine (supraglacial debris) (maximum age) can be ruled out. In these regards, the obtained exposure ages represent the time of deglaciation.

Discussion

Chronological correlation

Recent studies have evidenced the existence of post LGM glacial advances in the mountain of Turkey, Balkan and Carpathian (Fig. 5). Late-glacial glacial advances in Turkey were cosmogenically-dated at 14-16 ka and ~13 ka (Zahno *et al*. 2010; Sarikaya *et al.* 2008; Sarikaya *et al.* 2009; Ackar *et al.* 2014) (Fig. 6). Similar ages were also obtained in the Šara mountain chain (Kosovo), where a glacial advance was dated at ~14 ka, followed by a new advance at 11-12 ka (Kuhlemann *et al.* 2009). A Late-glacial phase was also dated in the south Carpathians (Retezat Mountains) at 14-17 ka (Reuther *et al.* 2007), followed by a more recent glacial advance (Fig. 6). These data match with the minimum ages obtained by secondary calcite in moraine deposits in the Massif of Orjen, Montenegro, where a Late-glacial phase older than 12-13 ka is proposed, along with a phase older than 8-9 ka BP (Hughes *et al.* 2011). A glacial advance at 14-19 ka (16.2 ± 2.7 ka) was documented in the Rila mountains (Bulgaria), although it has been interpreted as a late phase of the LGM (Kuhlemann *et al.* 2013) (Fig. 6). Recently, a Younger Dryas glacial phase (10-13 ka) was dated in the mountains of Peloponnesus (Mt Chelmos, Greece), where Oldest Dryas evidences seem to lack (Pope *et al*. 2017).

All these data converge in defining a glacial advance framed in the 14.5-17.5 ka interval, between the LGM and the Younger Dryas. Similar ages have also been reported from other circum-Mediterranean mountain ranges. These include the Alps (the Gschnitz stadial) (Ivy-Ochs *et al.* 2006), some of the main Spanish ranges (Palacio *et al.* 2016 and reference therein) and possibly the Central Apennines, where a stadial at ~15 ka has been hypothesised (Giraudi & Frezzotti 1997). These glacial advances throughout the Mediterranean are all chronologically linked to the climatic cold interval known as the Oldest Dryas, recognized in the oxygen isotope record of Greenland cores (GS-2a in the GRIP ice core) (Björk *et al.* 1998; Rasmussen *et al.* 2006).

In this framework, the frontal moraine in the Pelister mountain represents the first dated evidence of an Oldest Dryas glacial advance in the mountains of Macedonia. The high climatic instability that characterized this interval determined a number of glaciers' minor oscillations and the formation of moraine clusters in various regions (Ivy-Ochs *et al.* 2006; Darnault *et al.* 2012; Palacios *et al.* 2016). The few small moraines found immediately downvalley the dated Golemo Ezero moraine also, most likely, resulted from various minor advances within the Oldest Dryas interval. The moraine dated at ~15 ka represents the last advance before the Bolling/Allerod climatic amelioration.

Unlike other Balkan, Carpathians, Turkey mountains (Fig. 6) and Pindus mountain in Greece, there is no evidence of a Younger Dryas glacier advance in this Pelister's Veternica Valley, most likely because the lack of accommodation space for snow/ice deposition and because of limited elevations. In northern Greece, the Younger Dryas ELAs were 2,425 m a.s.l. according to Hughes *et al.* (2006b). In the Pelister mountain, which is in the rain shadow of the Pindus Mt-Albanian Alps, it is realistic to expect the ELA of Younger Dryas glaciers to be higher and certainly above the highest elevation of 2,420 m a.s.l. reached in the Veternica Valley above the dated moraine (Fig. 2). However, the presence of protalus ramparts nearby the Golemo Ezero moraine suggests that the top most part of the valley may have responded to the cold phase of the Younger Dryas with the formation of periglacial features.

ELA calculation and correlation across the Mediterranean region

At ~15 ka the glacier extended down to the Golemo Ezero moraine with a length of ~500 m, a maximum width of ~300 m and a thickness of up to 85 m. While the North-West side of the reconstructed glacier is flanked by the steep valley side, the South-East side appears to be less confined. This suggests that a second glacial mass could have been contemporaneously present in this area, partly in contact with the reconstructed glacier. This secondary glacier could be responsible for the deposition of the latero-frontal moraine system at the base of the eastern part of the cirque wall (Fig. 2).

The ELA calculation with the AABR method, adopting a ratio value of 1.6, yielded a value of 2,250 m asl. This value can be tentatively correlated with the ELAs obtained from reconstructed glaciers, associated to moraines dated to the Oldest Dryas, in other, circum-Mediterranean mountain ranges (Fig. 7). A summary plot of ELA vs. longitude (Fig. 8) shows how the ELA tends to be relatively consistent in the 7°-30° degree of longitude interval (varying in the 1,960-2,320 m asl altitudinal interval), with the notable exceptions of the Reovci glacier near the Adriatic coast of the Balkans (11 in Fig. 8) and of the Spain glaciers. The low value of ELA (1,425 m asl) of the Reovci Oldest Dryas glacier can be attributed to the role of the Adriatic Sea that generated a relatively high amount of humidity, which was eventually captured by the westernmost Balkan ranges (Hughes *et al.* 2010). The ELA of the Spain glaciers is on average higher than that of the other settings. For at least some of these Spain cases, it is possible that specific topoclimatic conditions controlled the increased ELA. For example, the high ELA value (2819 m asl) of the Seco

glacier in the Sierra Nevada (5 in Fig. 8) is probably due to the south aspect of the glacial basin. More in general, it must be taken into account that niche settings may tend to produce glaciers with ELAs that might not conform to the regional ELA. Indeed, there are examples of Mediterranean glaciers still surviving today below the regional snowline because of avalanching and windblown snow contribution (Hughes and Woodward 2017 and references therein).

Despite these exceptions, overall the ELA analysis demonstrates that the glacier in the Pelister Mountain responded to the Oldest Dryas cold interval in a way comparable to most of the central-eastern Mediterranean glaciers.

Correlations with climate proxies

Atmospheric circulation during the LGM, and, most probably, the Late-glacial, is thought to have been dominated by advection of cold air masses from the Atlantic Ocean over the Mediterranean region (Kuhlemann *et al.* 2008; Florinet & Schlüchter 2000). Indeed, various marine and continental climate proxies and palaeoenvironmental records registered the effect of changes in the North Atlantic thermohaline circulation during massive ice discharge, e.g. Heinrich event (Bar-Matthew *et al.* 1999; Bartov *et al.* 2003; Cacho *et al.* 2001; Fleitmann *et al*. 2009; Stanford *et al.* 2011) (Fig. 9a, b, c).

The fossiliferous contents of cores from Adriatic and North Aegean seas indicate that the Oldest Dryas has been a cold event that relevantly impacted on the conditions of the sea surface and terrestrial ecosystem (Combourieu *et al.* 1998; Siani *et al.* 2001; Kotthoff *et al.* 2011; Zonneveld 1996). Particularly, the planktonic foraminifera and dinocyst cold indicators (*Turborotalia Quinqueloba, Neogloboquadrina Pachyderma, Nemaosphaeropsis Labyrintus, Spiniferites Elongates*) suggests that the decline of Sea Surface Temperature (SST) culminated in a minimum at ~17 cal ka BP (Fig. 8d). Moreover, the fossil pollen assemblage in these cores indicates that the Oldest Dryas interval was characterized by pronounced dry condition, as evidenced by a great development of semi-desertic vegetation (*Artemisia*) and a scarce presence of trees. The pronounced dry condition is also demonstrated by the $\delta^{18}O$ signals recorded in speleothems (Fleitman *et al.* 2009) (Fig. 8c) and endogenic and biogenic carbonate deposits from lakes in the Mediterranean region (Roberts *et al.* 2008).

The palaeoenvironmental data nearer to the Pelister mountain are those inferred by the cores extracted at the bottom of the current Prespa and Ohrid lakes, along with that from

the now disappeared Lake Maliq (Fig. 1). The pollen assemblages are in agreement with a pronounced dryness during the Oldest Dryas, as evidenced by the dominance of cold-tolerant herbs and minimal occurrence of arboreal plants (cold steppa environment) (Aufgebauer *et al.* 2012; Wagner *et al.* 2010; Bordon *et al*. 2009; Panagiotopulus *et al*. 2014). Accordingly, the recorded, limited supply of Ca^{2+} and HCO_3^- ions to the lakes could be caused by inhibited soil formation and chemical weathering in the catchment associated with an open steppa vegetation (Aufgebauer *et al.* 2012; Panagiotopulus *et al.* 2013). A peak in the abundance curve of *Staurosirella Pinnata* (Fig. 8e), a typical glacial type species of diatom, correlates with a minimum of arboreal plants during the Oldest Dryas interval (Cvetkoska *et al.* 2015). The high content of Oldest Dryas clastic debris material (high K counts) (Fig. 8f) in the lake cores has been explained by a spring-summer water discharge linked to a seasonal melting of glaciers in the catchment (Aufgebauer *et al.* 2012; Damaschke *et al.* 2013). However, this high content of clastic material characterized both the LGM and the first part of the Late-glacial, thus suggesting that this seasonal glacier behavior was not restricted to the Oldest Dryas. Although the glaciers within the lake catchments did not reach the shores during the Oldest Dryas (Ribolini *et al.* 2011), a seasonal ice covering the lake (at least near the shores) should have been present, as testified by frequent Ice Rafted Debris (IRD) (Aufgebauer 2012; Wagner *et al.* 2010). Moreover, Mn Late-glacial peak in the Prespa Lake core (Fig. 8g) was associated to mixing phenomena in the water column, consistent with higher aeolian activity (Wagner *et al.* 2010). An increase in sand content suggesting dry conditions was also observed during the Oldest Dryas interval in the Lake Prespa core (Fig. 8h) (Aufgebauer *et al.* 2012).

Local Oldest Dryas temperature and precipitation were tentatively reconstructed using the fossil pollen assemblages of Lake Maliq (812 m asl, see Fig. 1 for location) (Bordon *et al*. 2009). An estimated mean annual air temperature (MAAT) from -3 to 1 °C (Fig. 8i) and mean annual precipitation lower than 400 mm were suggested. The reconstructed air temperature for the Oldest Dryas warmest month at Lake Maliq (8-10 °C) (Bordon *et al.* 2009) is partly in agreement with the Chironomid-inferred temperature of July (5.2-5.3 °C) calculated for the same interval at Lake Brazi (1,740 m asl), in the Southern Carpathians (Tóth *et al.* 2012) (Fig. 8j).

Local and regional palaeobotanical, geochemical and sedimentological data collectively converge in defining, directly or indirectly, a cold, dry and windy Oldest Dryas interval in the Mt Pelister region. More in general, the estimated dry conditions, together with the

correlation between the Pelister glacier advance and the H1 event, confirms that cold periods controlled by North Atlantic changes to the thermohaline circulation corresponded to aridity in the Mediterranean (Bartov *et al.* 2003; Roberts *et al.* 2008).

In the context of regional aridity, it is worth noting the relevant role of the mountain ranges facing the Adriatic Sea, which capture (today, and most likely in the past) most of the humidity contained in air masses sourced from the Adriatic Sea and further west, leaving the interior of the Balkan region relatively dry (Hughes *et al.* 2010).

Conclusion

The Oldest Dryas glacial advance is now dated for the first time in the mountain of Macedonia (Pelister Mountain) to the mean age of 15.24 ± 0.85 ka yr. This age adds a crucial piece to the puzzle of dated glacier advances in the Balkan Peninsula, and it represents a geographical bridge between these and other, nearby Mediterranean mountains, e.g. Turkey and Carpathian ranges. Furthermore, this exposure age fits well with other glacier advance dated in the Alps (Gschnitz advance) and the Balkan, Carpathians and Turkey mountains, thus drawing a coherent picture of glaciers response to the Oldest Dryas cold interval across the Mediterranean.

The ELA of the Oldest Dryas Pelister glacier is in good agreement with that of other circum-Mediterranean, reconstructed mountain glaciers of the same age. However, some relevant regional and inter-regional differences exist, indicating a glacier response to the Oldest Dryas cold period also modulated by the vicinity to source of atmospheric humidity, local topoclimatic factors, as well as diverse components in the atmospheric circulation. Palaeoenvironmental records provided by local lakes indicate that the Oldest Dryas has been a cold interval, characterized by a pronounced aridity.

This confirms how the interior of the Balkan region was more arid than the mountain ranges near the Adriatic coast, where the great amount of humidity sourced by the Adriatic Sea caused a pronounced depression of the ELA of local glaciers during the Oldest Dryas (Hughes *et al.* 2010).

The results of this work show how glacier advances may be incorporated in the record of the palaeoenvironmental data of the interior region of the Balkans, and cross-correlated with regional marine and terrestrial climate-proxy data. Moreover, the temporal relation between glacier advances in the Balkan region and changes in the thermohaline

circulation during the massive ice discharge event H1, confirms the climatic link between the pan Mediterranean regions and the North Atlantic Ocean.

Acknowledgments: We thank two reviewers and the editor P. Hughes for their insightful comments. We thank G. Chmiel and T. Woodruff (Universtity of Purde, Indiana) for their help with presenting the laboratory processing. We are in debt to S. Ivy-Ochs (ETH-Zürich, Switzerland) for her assistance in the exposure ages calculation. Funding for this work was provided to A. Ribolini and G. Zanchetta by the University of Pisa (ATENEO Project, Leader A. Ribolini, MIUR Project, Leader G. Zanchetta), to M. Spagnolo by the University of Aberdeen (College of Physical Sciences's Research Enhancement Fund) and the Leverhulme Trust (IAF-2016-001).

References

Akçar, N., Yavuz, V., Ivy-Ochs, S., Kubik, P.W, Vardar, M. & Schlüchter, C. 2007. Paleoglacial records from Kavron Valley, NE Turkey: Field and cosmogenic exposure dating evidence. *Quaternary International* **164-165**, 170−183.

Akçar, N., Yavuz V., Ivy-Ochs S., Reber R., Kubik P.W., Zahno C.& Schlüchter C. 2014. Glacier response to changes in atmospheric circulation in the eastern Mediterranean during the Last Glacial Maximum. *Quaternary Geochronology*, **19**, 27−41

Andonovski, T. & Milevski, I. 2001. *Geomorphological characteristics of Pelister Mountain.* Proceedings of DNU, Bitola, 23−32 (in Macedonian)

Arsovski M. 1997. *Tectonics of Macedonia*. Faculty of Geology and Mining, Stip. 306 pp. (in Macedonian).

Aufgebauer, A., Panagiotopoulos, K., Wagner, B., Schäbitz, F., Viehberg, F.A., Vogel, H., Zanchetta, G., Sulpizio, R., Leng, M.J. & Damaschke, M., 2012. Climate and environmental change in the Balkans over the last 17 ka recorded in sediments from Lake Prespa (Albania/F.Y.R. of Macedonia/Greece). *Quaternary International* **274**, 122–135

Balco, G., Briner, J., Finkel, R.C., Rayburn, J.A., Ridge, J.C. & Schaefer, J.M. 2009. Regional beryllium-10 production rate calibration for northeastern North America. *Quaternary Geochronology* **4**, 93−107.

Bar-Matthews, M., Ayalon, A., Kaufman, A. & Wasserburg, G.J. 1999. The Eastern Mediterranean paleoclimate as a reflection of regional events: Soreq Cave, Israel. *Earth and Planetary Science Letters* **166**, 85−95.

Bartov, Y., Goldstein, S.L., Stein, M. & Enzel, Y. 2003. Catastrophic arid episodes in the Eastern Mediterranean linked with the North Atlantic Heinrich events. *Geology* **31**, 439–442.

Björck, S., Walker, M.J.C., Cwynar, L.C., Johnsen, S., Knudsen, K.L., Lowe, J.J., Wohlfarth, B. & Members, I. 1998. An event stratigraphy for the Last Termination in the north Atlantic region based on the Greenland ice-core record: a proposal by the INTIMATE group. *Journal of Quaternary Science* **13**, 283−292.

Bordon, A., Peyron, O., Lézine, A.-M., Brewer, S. & Fouache, E. 2009. Pollen-inferred Late-Glacial and Holocene climate in southern Balkans (Lake Maliq). *Quaternary International* **200**, 19−30.

Burchfiel, B.C,, Dumurdzanov, N., Serafimovski T. & Nakov, R. 2004. *The Southern Balkan Cenozoic Extensional Region and its relation to extension in the Aegean Realm*. Geological Society American Abstract with Programs **36**, 5, 52.

Cacho, I., Grimalt, J.O., Canals, M., Sbaffi, L., Shackleton, N.J., Schönfeld, J.& Zahn, R. 2001. Variability of the western Mediterranean Sea surface temperature during the last 25,000 years and its connection with the Northern Hemisphere climatic changes. *Paleoceanography* **16,** 40−52.

Carrasco, R.M., Pedraza, J., Domínguez-Villar, D., Willenbring, J. K. & Villa, J. 2015. Sequence and chronology of the Cuerpo de Hombre paleoglacier (Iberian Central System) during the last glacial cycle. *Quaternary Science Reviews,* **129**, 163−177.

Clark, P. U., Shakun, J.D., Baker, P.A., Bartlein, P.J., Brewer, S., Brook, Ed., Carlson, A.E., Chenh, H., Kaufman, D.S., Liu, Z., Marchitto, T.M., Mixd, A.C., Morrill, C., Otto-Bliesner. B.T., Pahnke, K., Russell, J.M., Whitlock, C., Adkins, J.F., Blois, J.L., Clark, J., Colman, S.M., Curry, W.B., Flower, B.P., He, F., Johnson T.C., Lynch-Stieglitz, J., Markgraf, V., McManus, J., Mitrovica, J.X., Moreno, P.I. & Williams, J.W. 2012. *Global climate evolution during the last deglaciation.* Proceedings of the National Academy of Sciences of the United States of America, **109**, E1134–E1142.

Combourieu N. Paterne M., Turon J.L., Siani G. 1998. A high-resolution record of the last deglaciation in the central Mediterranean Sea: palaeovegetation and palaeohydrological evolution. *Quaternary Science Reviews*, **17**, 303−317.

Cvetkoska A., Levkov S., Reed J., Wagner B., Panagiotopoulos K., Leng M.J., Lacey J.H. 2015. Quaternary climate change and Heinrich events in the southern Balkans: Lake Prespa diatom palaeolimnology from the last interglacial to present. *Journal of Paleolimnology,* **53**, 215−231.

Damaschke, M., Sulpizio, R., Zanchetta, G., Wagner, B., Böhm, A., Nowaczyk, N., Rethemeyer, J. & Hilgers, A. 2013. Tephrostratigraphic studies on a sediment core from Lake Prespa in the Balkans. *Climate of the Past*, **9**, 267−287.

Darnault, R., Rolland, Y., Braucher, R., Bourlès,D., Revel, M., Sánchez, G., Bouissou, S. & 2012. Timing of the last deglaciation revealed by receding glaciers in the Alpine-scale: impact on mountain geomorphology. *Quaternary Science Reviews*, **31**,127–142.

Desilets, D. & Zreda, M., 2003. Spatial and temporal distribution of secondary cosmic-ray nucleon intensities and applications to in-situ cosmogenic dating. *Earth and Planetary* Science Letters, 206, 21–42.

Desilets, D., Zreda, M. & Prabu, T. 2006. Extended scaling factors for in situ cosmogenic nuclides: New measurements at low latitude. *Earth and Planetary Science Letters*, **246**, 265–276.

Dunai, T., 2001. Influence of secular variation of the magnetic field on production rates of in situ produced cosmogenic nuclides. *Earth and Planetary Science Letters*, **193**, 197–212.

Dunne, J., Elmore, D. & Muzikar, P. 1999. Scaling factors for the rates of production of cosmogenic nuclides for geometric shielding and attenuation at depth on sloped surfaces. *Geomorphology,* **27**, 3–11.

Federici, P.R., Granger, D.E., Pappalardo, M., Ribolini, A., Spagnolo, M., & Cyr, A.J. 2008. Exposure age dating and Equilibrium Line Altitude reconstruction of an Egesen moraine in the Maritime Alps, Italy. *Boreas,* **37**, 245−253.

Federici, P.R., Granger, D.E., Ribolini, A., Spagnolo, M., Pappalardo, M. & Cyr, A.J. 2012. Last Glacial Maximum and the Gschnitz stadial in the Maritime Alps according to 10Be cosmogenic dating. *Boreas*, **41**, 277−291.

Federici, P.R., Ribolini, A. & Spagnolo, M. 2017. Glacial history of the Maritime Alps from the Last Glacial Maximum to the Little Ice Age. *In:* Hughes, P. D. & Woodward, J. C. (eds). *Quaternary Glaciation in the Mediterranean Mountains*. Geological Society, London, Special Publications, **433**, 137–159.

Fleitmann D. Cheng H., Badertscher S., Edwards R.L., Mudlsee M., Gökturk O.M., Fankhauser A., Pickering R., Raible C.C., Matter A., Kramers J., & Tüysuz O. 2009. Timing and climatic impact of Greenland interstadials recorded from northern Turkey. *Geophysical Research Letters,* **36**, http://doi.org/10.1029/2009GL040050.

Florineth D. & Schlüchter C. 2000. Alpine evidence for atmospheric circulation patterns in Europe during the Last Glacial Maximum. *Quaternary Research*, **54**, 295–308.

Giraudi, C., & Frezzotti, M. 1997. Late Pleistocene glacial events in the Central Apennines, Italy. *Quaternary Research*, **48**, 280−290.

Hijmans, R.J., Cameron, S.E., Parra, J.L., Jones, P.G. & Jarvis, A. 2005. Very high resolution interpolated climate surfaces for global land areas. *International Journal of Climatology*, **25**, 1965−1978

Hoffmann, N. 2013. The active tectonic landscape of Lake Ohrid (FYR of Macedonia/Albania). *Annals of Geophysics*, **56**, 6, S0678; http://doi.org/10.4401/ag-6254

Hollis, G.E., & Stevenson, A.C. 1997. The physical basis of the Lake Mikri Prespa systems: geology, climate, hydrology and water quality. *Hydrobiologia* **351**,1−19.

Hughes, P.D. & Gibbard, P.L. 2015. A stratigraphical basis for the Last Glacial Maximum (LGM). *Quaternary International*, **383**, 174−185.

Hughes, P.D. & Woodward, J.C. 2008. Timing of glaciation in the Mediterranean mountains during the last cold stage. *Journal of Quaternary Science*, **23**, 575−588.

Hughes, P.D. & Woodward, J.C. 2017. Quaternary glaciation in the Mediterranean: a new synthesis. In: Hughes, P.D. & Woodward, J.C. (eds) *Quaternary Glaciation in the Mediterranean Mountains*. Geological Society, London, Special Publications, **433**, 1-23. https://doi.org/10.1144/SP433.14

Hughes, P.D., Woodward, J.C. & Gibbard, P.L. 2006a. Quaternary glacial history of the Mediterranean mountains. *Progress in Physical Geography* **30**, 334−364.

Hughes, P.D., Woodward, J.C. & Gibbard, P.L. 2006b. The last glaciers of Greece. Zeitschrift für Geomorphologie, **50**, 37–61.

Hughes, P.D., Woodward, J.C., Gibbard, P.L., Macklin, M.G., Gilmour, M.A. & Smith, G.R. 2006. The glacial history of the Pindus mountains, Greece. *Journal of Geology,* **114**, 413−434.

Hughes, P.D., Woodward, J.C., van Calsteren, P.C., Thomas, L.E. & Adamson, K.R. 2010. Pleistocene ice caps on the coastal mountains of the Adriatic Sea. *Quaternary Science Reviews*, **29**, 3690−3708.

Hughes P.D., Woodward J.C., van Calsteren P.C. & Thomas L.E. 2011. The glacial history of the Dinaric Alps, Montenegro. *Quaternary Science Reviews*, **30**, 3393−3412.

Hughes, P.D. & Gibbard, P.L. 2015. A stratigraphical basis for the Last Glacial Maximum (LGM). *Quaternary International*, **35**, 174-185

Ivy-Ochs, S., Kerschner, H., Kubik, P.W. & Schlüchter, C. 2006. Glacier response in the European Alps to Heinrich Event 1 cooling: the Gschnitz stadial. *Journal of Quaternary Science*, **21**, 115−130.

Ivy-Ochs, S., Kerschner, H., Maisch, M., Christl, M., Kubik, P.W. & Schluchter, C. 2009. Latest Pleistocene and Holocene glacier variations in the European Alps. *Quaternary Science Reviews*, **28**, 2137−2149.

Kolčakovski D. 1996. *Morphogenetic processes and their relief forms on the high mountain regions on the mountains Jablanica, Stogovo, Stara Galicica and Pelister*. PhD thesis

Kotthoff, U., Koutsodendris, A., Pross, J., Schmiedl, G., Bornemann, A., Kaul, C., Marino, G., Peyron, O. & Schiebel, R. 2011. Impact of Lateglacial cold events on the northern

Aegean region reconstructed from marine and terrestrial proxy data. *Journal of Quaternary Science*, **26**, 86−96.

Kuhlemann, J., Rohling, E.J., Krumrei, I., Kubik, P., Ivy-Ochs, S. & Kucera, M. 2008. Regional synthesis of Mediterranean atmospheric circulation during the last glacial maximum. *Science* **321**, 1338−1340.

Kuhlemann, J., Milivojevic, M., Krumrei, I., & Kubik, P.W. 2009. Last glaciation of the Sara range (Balkan peninsula): Increasing dryness from the LGM to the Holocene. Austian *Journal of Earth Science*, **102**, 146−158.

Kuhlemann J. Gachev E., Gikov A., Nedkov S., Krumrei I. & Kubik P. 2013. Glaciation in the Rila mountains (Bulgaria) during the Last Glacial Maximum. *Quaternary International* **293**, 51−62.

Lal, D. 1991. Cosmic-ray labeling of erosion surfaces e in-situ nuclide production rates and erosion models. *Earth Planetary Sciences Letters*, **104**, 424-439.

Lifton, N., Bieber, J., Clem, J., Duldig, M., Evenson, P., Humble, J. & Pyle, R. 2005. Addressing solar modulation and long-term uncertainties in scaling secondary cosmic rays for in situ cosmogenic nuclide applications. *Earth and Planetary Science Letters*, **239**, 140–161.

Lilienberg D.A. 1968. The main regularities in recent movements in the central parts of the Balkan peninsula (On the example of Macedonia). *Studia Geophysica et Geodaetica*, **12**, 163−178.

Lionello, P., Malanotte-Rizzoli, P. & Boscolo, R., 2006. *Mediterranean Climate Variability*. Elsevier, Amsterdam.

Menković, L., Marković, M., Cupković, T., Pavlović, R., Trivić, B. & Banjać, N. 2004. Glacial morphology of Serbia Yugoslavia, with comments on the Pleistocene glaciation of Montenegro, Macedonia and Albania. *In*: Ehlers, J., Gibbard, P.L. (eds) *Quaternary Glaciations-Extent and Chronology. Part I: Europe*, Elsevier, 488.

Milevski I., 2015. General geomorphological characteristics of the Republic of Macedonia. *Geographical Reviews*, **48**, 5−25.

Nishiizumi, K., Imamura, M., Caffee, M., Southon, J.R., Finkel, R.C. & McAnich, J. 2007. Absolute calibration of ^{10}Be AMS standards. *Nuclear Instruments and Methods in Physics Research*, B, **258**, 403-413.

Oerlemans, J., 2005. Extracting a climate signal from 169 glacier records. *Science*, **308**, 675−677.

Osmaston, H.A. 2005. Estimates of glacier equilibrium line altitudes by the Area_Altitude, the Area_Altitude Balance Ratio and the Area_Altitude Balance Index methods and their validation. *Quaternary International,* **138–139**, 22–31.

Palacios, D. Andrés, N., Marcos, J. & Vázquez-Selem, L. 2012. Maximum glacial advance and deglaciation of the Pinar Valley (Sierra de Gredos, Central Spain) and its significance in the Mediterranean context. *Geomorphology*, **177-178**, 51−61.

Palacios, D., Gómez-Ortiz, A., Andrés N., Vázquez-Selem, L., Salvador-Franch, F. & Oliva, M. (2015). Maximum extent of Late Pleistocene glaciers and last deglaciation of La Cerdanya mountains, Southeastern Pyrenees. *Geomorphology*, **231**, 116−129.

Palacios, D., Andrés N., López-Moreno, J.I. & García-Ruiz, J.M. 2015. Late Pleistocene deglaciation in the upper Gállego Valley, central Pyrenees. *Quaternary Research*, **83**, 397−414.

Palacios, D., Gómez-Ortiz, A., Andrés N., Salvador, F. & Oliva, M. 2016. Timing and new geomorphologic evidence of the last deglaciation stages in Sierra Nevada (southern Spain). *Quaternary Science Reviews*, **150**, 110−129.

Palacios D., De Andrés N., Gòmez-Ortiz A. & García-Ruiz G. 2017. Evidence of glacial activity during the Oldest Dryas in the Mountain of Spain. *In:* Hughes P. and Woodward J. *Quaternary glaciation in the Mediterranean Mountains*. Geological Society of London, Special Publication, **433**, http://doi.org/10.1144/SP433.10

Pallas, Rodés, Á., Braucher, R., Bourlès, D., Delmas, M., Calvet, M. & Gunnell, Y. 2010. Small, isolated glacial catchments as priority targets for cosmogenic surface exposure dating of Pleistocene climate fluctuations, southeastern Pyrenees. *Geology,* **38**, 89−894.

Panagiotopoulos, K., Aufgebauer, A., Schäbitz, F.& Wagner, B. 2013. Vegetation and climate history of the Lake Prespa region since the Lateglacial. *Quaternary International*, **293**, 157−169.

Panagiotopoulos K, Böhm A., Leng M.J., Wagner B. & Schäbitz F. 2014. Climate variability over the last 92 ka in SW Balkans from analysis of sediments from Lake Prespa. *Climate of the Past*, **10**, 643–660

Pellitero, R., Rea, B.R., Spagnolo, M., Bakke, J., Hughes, P., Ivy-Ochs, S., Lukas, S. & Ribolini, A. 2015. A GIS tool for automatic calculation of glacier equilibrium-line altitudes. *Computers & Geosciences*, **82**, 55−62

Pellitero-Ondicol, R., Rea, BR., Spagnolo, M., Bakke, J., Ivy-Ochs, S., Frew, CR., Hughes, P., Ribolini, A., Lukas, S. & Renssen, H. 2016. Glare, a GIS tool to reconstruct the 3D surface of palaeoglaciers. *Computers & Geosciences*, **94**, 77−85.

Pope, R.J., Hughes, P.D. & Skourtsos, E. 2015. Glacial history of Mt Chelmos, Peloponnesus, Greece. In: Hughes, P.D. & Woodward, J.C. (eds) *Quaternary Glaciation in the Mediterranean Mountains*. Geological Society, London, Special Publications, **433**, 211-236. https://doi.org/10.1144/SP433.11

Rasmussen, S.O., Andersen, K.K., Svensson, A.M., Steffensen, J.P., Vinther, B.M., Clausen, H.B., Siggaard-Andersen, M.L., Johnsen, S.J., Larsen, L.B., Dahl-Jensen, D., Bigler, M., Röthlisberger, R., Fischer, H., Goto-Azuma, K., Hansson, M.E. & Ruth, U. 2006. A new Greenland ice core chronology for the last glacial termination. *Journal of Geophysical Results*, **111**, D06102. http://dx.doi.org/10.1029/02005JD006079.

Rasmussen, S. O., Bigler, M., Blockley, S. P., Blunier, T., Buchardt, S. L.,. Clausen, H. B., Cvijanovic, I., Dahl-Jensen, D., Johnsen, S. J. , Fischer, H., Gkinis, V., Guillevic, M., Hoek, W. Z., Lowe, J. J., Pedro, J. B., Popp T., Seierstad, I. K., Steffensen, J. P., Svensson, A. M., Vallelonga, P., Vinther, B.M., Walker, M.J.C., Wheatley, J.J. & Winstrup, M. 2014. A stratigraphic framework for abrupt climatic changes during the Last Glacial period based on three synchronized Greenland ice-core records: refining and extending the INTIMATE event stratigraphy. *Quaternary Science Reviews* , **106**, 14−28.

Rea, B.R. 2009. Defining modern day Area-Altitude Balance Ratios (AABRs) and their use in glacier-climate reconstructions. *Quaternary Science Reviews*, **28**, 237–248.

Renssen, H. & Isarin, R.F.B. 2001.The two major warming phases of the last deglaciation at ~14.7 and ~11.5 ka cal BP in Europe: climate reconstructions and AGCM experiments. *Global and Planetary Change,* **30**,117–153.

Reuther, A.U., Urdea, P., Geiger, C., Ivy-Ochs, S., Niller, H.-P., Kubik, P.W. & Heine, K. 2007. Late Pleistocene glacial chronology of the Pietrele Valley, Retezat Mountains, Southern Carpathians constrained by 10Be exposure ages and pedological investigations. *Quaternary International,* **164-165**, 151−169.

Ribolini, A., Isola, I., Zanchetta, G., Bini, M. & Sulpizio, R. 2011. Glacial features on the Galicica Mountains, Macedonia: Preliminary report. *Geografia Fisica e Dinamica Quaternaria,* **34**, 247−255.

Roberts, N., Jones, M.D., Benkaddur, A., Eastwood, W.J., Filippi, M.L., Frogley, M.R., Lamb, H.F., Leng, M.J., Reed, J.M., Stein, M., Stevens, L., Valero-Garcè, B. &

Zanchetta, G. 2008. Stable isotope records of Late Quaternary climate and hydrology from Mediterranean lakes: the ISOMED synthesis. *Quaternary Science Review*, **27**, 2426−2441.

Rodríguez-Rodríguez, L., Jiménez-Sánchez , M., Domínguez-Cuesta, M.J., Rinterknecht, V., Pallàs, R. & Bourlè D. 2016. Chronology of glaciations in the Cantabrian Mountains (NW Iberia) during the Last Glacial Cycle based on in situ-produced 10Be. *Quaternary Science Reviews,* **138**, 31−48.

Ruszkiczay-Rüdiger, Z., Kern, Z., Urdea, P., Braucher, R., Madarász, B. Schimmelpfennig I., & ASTER Team, 2015. Revised deglaciation history of the Pietrele-Stânişoara glacial complex, Retezat Mts, Southern Carpathians, Romania. *Quaternary International*, **415**, 216−229.

Sarıkaya, M.A., Zreda, M., Çiner, A. & Zweck, C. 2008. Cold and wet Last Glacial Maximum on Mount Sandiras, SW Turkey, inferred from cosmogenic dating and glacier modelling. *Quaternary Science Reviews*, **27**, 769−780.

Sarıkaya, M.A., Zreda, M. & Çiner, A. 2009. Glaciations and paleoclimate of Mount Erciyes, central Turkey, since the Last Glacial Maximum, inferred from 36Cl dating and glacier modeling. *Quaternary Science Reviews*, **28**, 2326−2341.

Siani, G., Paterne, M., Michel, E., Sulpizio, R., Sbrana, A., Arnold, M. & Haddas, G. 2001. Mediterranean Sea surface radiocarbon reservoir age changes since the Last Glacial Maximum. *Science,* **294**, 1917–1920.

Stanford, J.D., Rohling, E.J., Bacon, S., Roberts, A.P., Grousset, F.E. & Bolshaw, M. 2011. A new concept for the paleoceanographic evolution of Heinrich event 1 in the North Atlantic. *Quaternary Science Reviews*, **30**, 1047–1066.

Stojadinović, Č. 1970. *Geologic-geomorphic evolution of the relief of Pelister*. Proceedings of the Symposium for Molika, Skopje, 39–48 (in Macedonian).

Stone, J.O., 2000. Air pressure and cosmogenic isotope production. Journal of Geophysical Results- Solid Earth, **105**, 23753-23759.

Tóth, M., Magyari, E.K., Brooks, S.J., Braun, M., Buczkó, K., Bálint, M. & Heiri, O. 2012. A chironomid-based recosntruction of late glacial summer temperatures in the southern Carpathians, Romania*). Quaternary Research*, **77**, 122−131.

Wagner, B., Vogel, H., Zanchetta, G. & Sulpizio, R. 2010. Environmental changes on the Balkans recorded in the sediments from lakes Prespa and Ohrid. *Biogeosciences,* **7**, 3187−3198.

Zahno, C., Akçar, N., Yavuz, V., Kubik, P.W. & Schlüchter, C. 2009. Surface exposure dating of Late Pleistocene glaciations at the Dedegol mountains (Lake Beysehir, SW Turkey). *Journal of Quaternary Science,* **24**, 1016−1028.

Zahno, C., Akçar, N., Yavuz, V., Kubik, P.W. & Schlüchter, C. 2010. Chronology of Late Pleistocene glacier variations at the Uludag Mountain, NW Turkey. *Quaternary Science Reviews*, **29**, 1173−1187.

Zonneveld, K. A.F. 1996. Palaeoclimatic reconstruction of the last deglaciation (18-8 ka B.P.) in the Adriatic Sea region; a land-sea correlation based on palynological evidence. *Palaeogeography, Palaeoclimatology, Palaeoecology*, **122**, 89−106.

sample	Lat (° N)	Long (° E)	Elev (m asl)	Atm Press	Sample thick. (cm)	Sample density $grcm^{-3}$	Shield corr.	Er. rate	10Be conc (at gr^{-1})	Uncert. 10Be (at gr^{-1})	10Be stand.
EZ1	40.5809	21.122	2215	Std	2	2.7	0.991	0	302700	8783	07KNSTD
EZ2	40.9693	21.206	2215	Std	2	2.7	0.991	0	315600	7691	07KNSTD
EZ3	40-9636	21.206	2213	Std	2	2.7	0.994	0	307900	9006	07KNSTD

Table 1. *^{10}Be exposure ages of the Golemo Ezero moraine, with sample name, coordinates and elevation, and the concentration of ^{10}Be measured at the PRIME Lab against standard 07KNSTD. The evaluated thickness and shielding factors are reported.*

(a)

Sample name	Thickness scaling factor	Shielding factor	Prod. rate (muons) (atoms/g/yr)	Int. uncertainty (yr)	Exp.age (yr)	Ext. uncertainty (yr)	Prod. rate (spallation) (atoms/g/yr)
EZ1	0,9833	0,991	0,369	443	15034	857	20,09
EZ2	0,9833	0,991	0,37	386	15560	852	20,26
EZ3	0,9833	0,994	0,369	451	15149	865	20,29

(b)

Scaling scheme for spallation:	Desilets *et al.* (2003,2006)		Dunai (2001)		Lifton *et al.* (2005)		Time-dependent Lal (1991)/Stone (2000)	
Sample name	Exp age (yr)	Ext uncertainty (yr)	Exp. age (yr)	Ext. uncertainty (yr)	Exp. age (yr)	Ext. uncertainty (yr)	Exp. age (yr)	Ext. uncertainty (yr)
EZ1	14302	825	14498	837	14222	819	14847	851
EZ2	14750	817	14923	828	14666	812	15346	845
EZ3	14383	831	14563	843	14302	825	14956	859

Table 2. *Details of exposure ages calculation.* ***(a)****: exposure ages calculated with a constant production rate model, scaling system for spallation of Lal (1991) and Stone (2000); the internal uncertainty (analytical uncertainties which are dominated by AMS uncertainties) and the external uncertainty (both analytical and production rate uncertainties) are given.* ***(b)****: exposure ages calculated with a time-varying production models.*

Figure captions

Fig. 1. Hillshade model of the Lake Ohrid and Lake Prespa region. The study area on the Pelister mountain range is indicated.

Fig. 2. Geomorphological map of the upper Veternica Valley. 1: bedrock; 2: glacial deposit; 3: moraine ridge; 4: glacial cirque; 5: block field; 6: protalus rampart; 7: slope debris; 8: rockfall; 9: debris flow fan.

Fig. 3. Principal geomorphological features of the upper Veternica Valley. a, b: the lowermost frontal moraines in the studied area; c: the uppermost frontal moraine in the studied area (Golemo Ezero moraine) with samples locations indicated; d: protalus ramparts on the western flank of the valley. See also Figure 2.

Fig. 4. Sampled boulders on the top of the Golemo Ezero moraine. Sampling strategy favored flat-topped boulder emerging for some decimeters from the moraine crest.

Fig. 5. Locations in the Balkans, Carpathians and Turkey mountains where moraines were dated according to cosmogenic isotopes. 1: Šara mountain chain (Balkans, Kosovo) (^{10}Be) (Kuhlemann *et al*. 2009); 2: Pelister mountain (Balkans, Macedonia) (this work); 3: Rila mountains (Carpathian, Bulgaria) (^{10}Be) (Kuhlemann *et al.* 2013); 4: Retezat mountains (Carpathians, Romania) (^{10}Be) (Reuther *et al.* 2007); 5: Sandiras Mountains (SW Turkey) (^{36}Cl) (Sarikaya *et al.* 2008); 6: Uludag Mountain (NW Turkey) (^{10}Be) (Zahno *et al.* 2010); 7: Erciyes Mountain (centre-south Turkey) (^{36}Cl) (Sarikaya *et al.* 2009); 8: Erciyes Mountain (centre-south Turkey) (^{36}Cl) (Sarikaya *et al.* 2009); 9: Uludag mountain (NW Turkey) (^{10}Be) (Ackar *et al.* 2014); 10: Dodegol mountain (SW Turkey) (^{10}Be) (Zahno *et al.* 2009); 11: Kaçkar Mountain-Kavron Valley (NE Turkey) (^{10}Be) (Ackar *et al.* 2007).

Fig. 6. Plot showing the exposure age obtained in the Pelister mountain (Golemo Ezero moraine) compared with the (averaged) exposure ages found the Balkans, Carpathians and Turkey mountains. For site details and references see Fig. 4.

Fig. 7. Locations in the circum-Mediterranean mountains where ELA were recalculated. 1: Cuerpo de Hombre glacier (Central range, Spain) (Carrasco 2015; 2: Asuente glacier (Cantabrian range, Spain) (Rodriguez-Rodriguez 2016); 3: Pinar glacier (Central range, Spain) (Palacios 2012); 4: Hoya Mora glacier (Sierra Nevada, Spain) (Palacios *et al.*

2016); 5: Seco glacier (Sierra Nevada, Spain) (Palacios *et al.* 2016); 6: Piniecho glacier (Pyrenees, Spain) (Palacios *et al.* 2015); 7: Aranser glacier (Pyrenees, Spain) (Palacios *et al.* 2014); 8: Orri glacier (Pyrenees, Spain) (Pallas *et al.* 2010; 9: Gesso glacier (Maritime Alps, NW Italy) (Federici *et al.* 2017); 10: Aquila glacier (three reconstructed glaciers in the same valley) (Apennines, central Italy) (Giraudi & Frezzotti 1997); 11: Reovci glacier (Balkans, Montenegro) (Hughes *et al.* 2010); 12: Pelister glacier (Balkans, Macedonia) (this work); 13: Pietrele glacier (south Carpathians, Romania) (Ruszkiczay-Rudiger *et al*. 2015); 14: Rila glacier (Balkans, Bulgaria) (Kulhemann *et al.* 2013); 15: Sandiras glacier (Taurus mountain, SW Turkey) (Sarikaya *et al.* 2008); 16: Karagol glacier (Uludag mountain, NW Turkey) (Zahno *et al.* 2010).

Fig. 8. ELA of Oldest Dryas glaciers vs. longitude of the principal circum-Mediterranean mountains. For site details and references see Fig. 7.

Fig. 9. Climate proxy data and palaeoenvironmental records compared with glacial advances in the Balkan and Carpathian mountains. (**a**): $\delta^{18}O$ recorded in the Greenland ice core (GRIP) (Rasmussen et al., 2006); (**b**): alkenone-based Sea Surface Temperature in the Alboran Sea (Cacho *et al.* 2001); (**c**): $\delta^{18}O$ record of speleothem from the Sofular cave (Turkey) (Fleitmann *et al*. 2009); (**d**): planktonic foraminifera-based Sea Surface Temperature in the Adriatic Sea (Siani *et al.* 2001); (**e**): record of *Staurosirella Pinnata diatom* in the Prespa Lake (Cvetkoska *et al.* 2015); (**f**): K counts (peaks indicates increase in clastic debris input) in the Prespa Lake (Damaschke *et al.* 2013); (**g**): Mn record in the Prespa Lake core (peaks are associated to mixing phenomena in the water column, consistent with increased aeolian activity) (Wagner *et al.* 2010); (**h**): sand content in the Prespa lake core (Aufgebauer *et al.* 2012); (**i**): Mean Annual Air Temperature based on pollen assemblage at Lake Maliq (see Fig. 1 for location) (Bordon *et al.* 2009); (**j**): Chironomid-inferred air temperature of July at Lake Brazi (Southern Carpathians) (Tóth *et al.* 2012); (**k**): exposure ages of stadial moraines in the Balkans and Carpathians, 1) Šara mountain chain (Balkans, Kosovo) (Kuhlemann *et al.* 2009), 2) Rila mountains (Carpathian, Bulgaria) (Kuhlemann *et al.* 2013), 3) Rezetat mountains (Carpathians, Romania) (Reuther *et al.* 2007), 4) Rezetat mountains (Carpathians, Romania) (Reuther *et al.* 2007), 5) Pelister Mountain (this work). Timing of H_0 and H_1 Heinrich events according to Rasmussen *et al.* 2014.

sample	Lat (° N)	Long (° E)	Elev (m asl)	Atm Press	Sample thick. (cm)	Sample density $grcm^{-3}$	Shield corr.	Er. rate	10Be conc (at gr^{-1})	Uncert. 10Be (at gr^{-1})	10Be stand.
EZ1	40.5809	21.122	2215	Std	2	2.7	0.991	0	302700	8783	07KNSTD
EZ2	40.9693	21.206	2215	Std	2	2.7	0.991	0	315600	7691	07KNSTD
EZ3	40-9636	21.206	2213	Std	2	2.7	0.994	0	307900	9006	07KNSTD

Table 1. *^{10}Be exposure ages of the Golemo Ezero moraine, with sample name, coordinates and elevation, and the concentration of ^{10}Be measured at the PRIME Lab against standard 07KNSTD. The evaluated thickness and shielding factors are reported.*

(a)

Sample name	Thickness scaling factor	Shielding factor	Prod. rate (muons) (atoms/g/yr)	Int. uncertainty (yr)	Exp.age (yr)	Ext. uncertainty (yr)	Prod. rate (spallation) (atoms/g/yr)
EZ1	0,9833	0,991	0,369	443	15034	857	20,09
EZ2	0,9833	0,991	0,37	386	15560	852	20,26
EZ3	0,9833	0,994	0,369	451	15149	865	20,29

(b)

Scaling scheme for spallation:	Desilets and others (2003,2006)		Dunai (2001)		Lifton and others (2005)		Time-dependent Lal (1991)/Stone (2000)	
Sample name	Exp age (yr)	Ext uncertainty (yr)	Exp. age (yr)	Ext. uncertainty (yr)	Exp. age (yr)	Ext. uncertainty (yr)	Exp. age (yr)	Ext. uncertainty (yr)
EZ1	14302	825	14498	837	14222	819	14847	851
EZ2	14750	817	14923	828	14666	812	15346	845
EZ3	14383	831	14563	843	14302	825	14956	859

Table 2. *Details of exposure ages calculation.* ***(a)****: exposure ages calculated with a constant production rate model, scaling system for spallation of Lal (1991) and Stone (2000); the internal uncertainty (analytical uncertainties which are dominated by AMS uncertainties) and the external uncertainty (both analytical and production rate uncertainties) are given.* ***(b)****: exposure ages calculated with a time-varying production models.*

Figure 1

Click here to download Figure FIG_1_LR.pdf

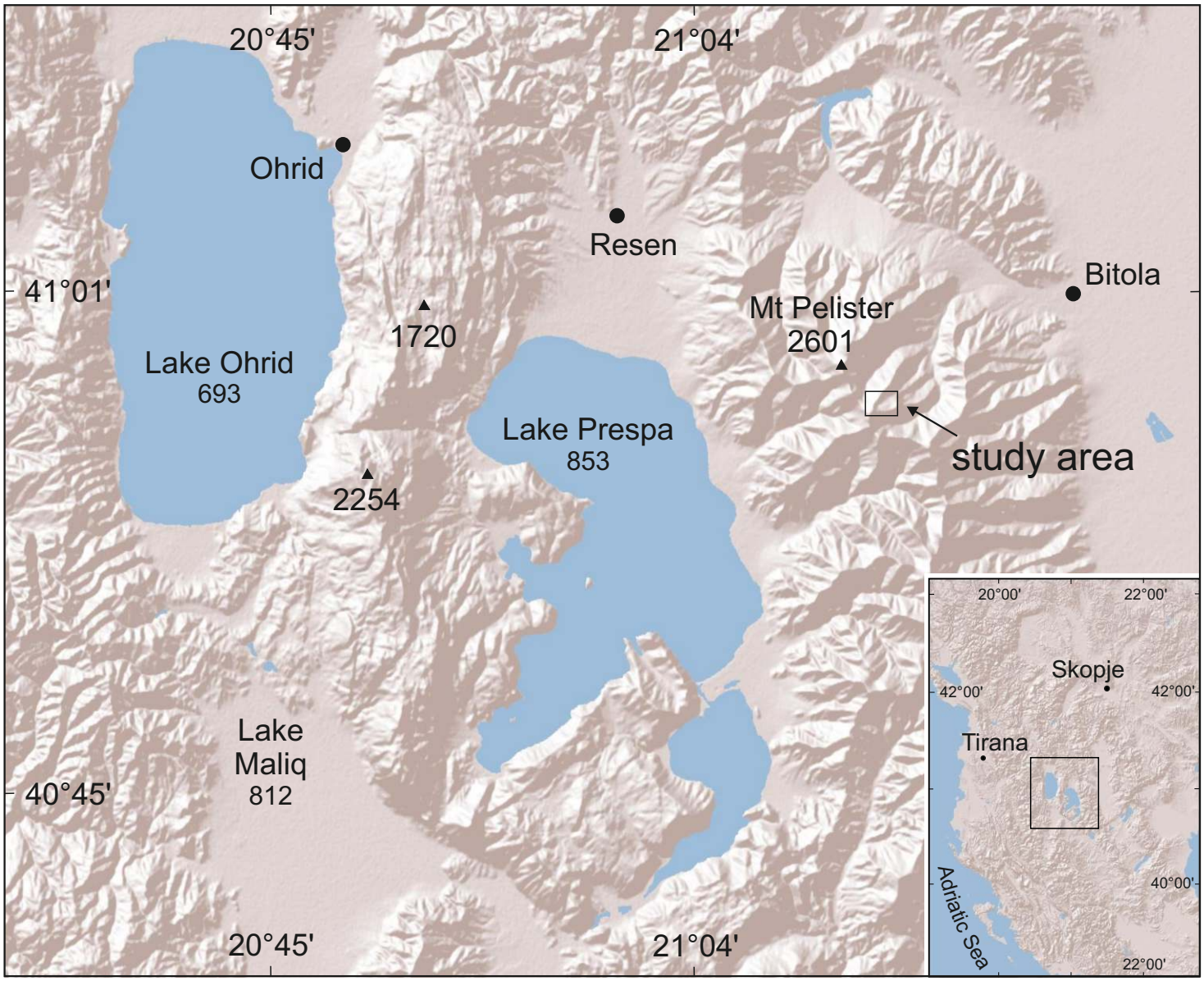

Figure 2

Click here to download Figure FIG_2_LR.pdf

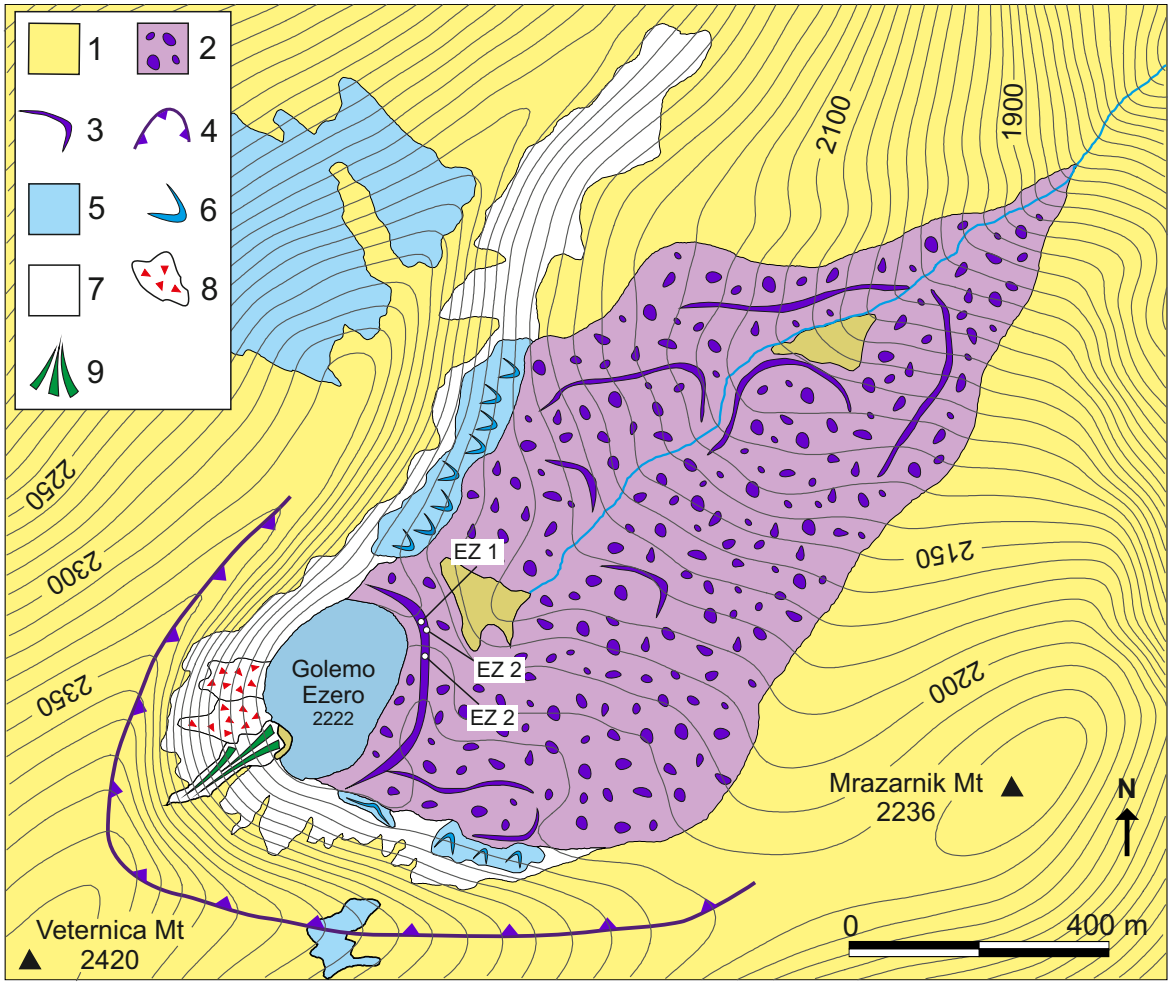

Figure 3

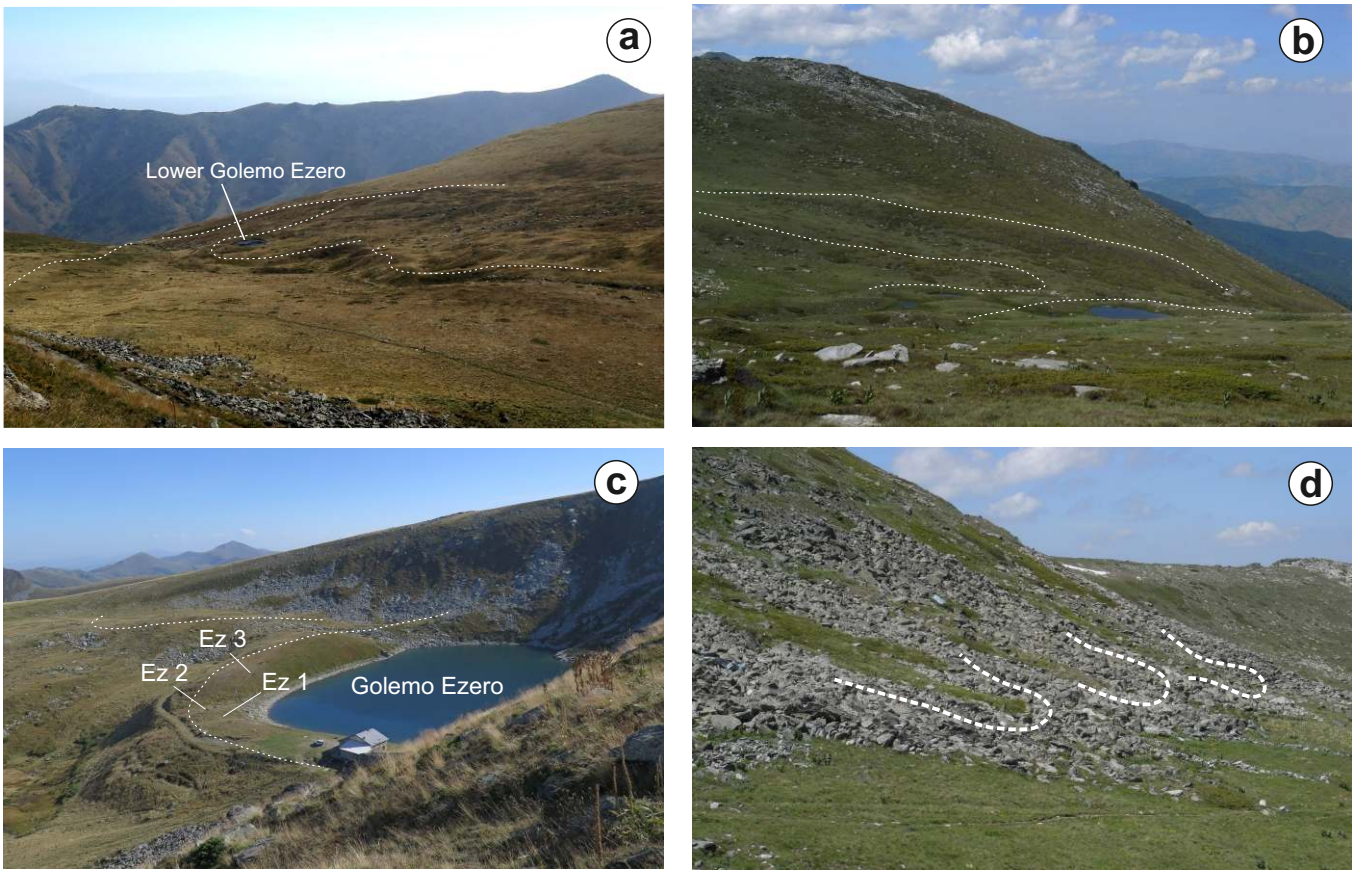

Figure 4

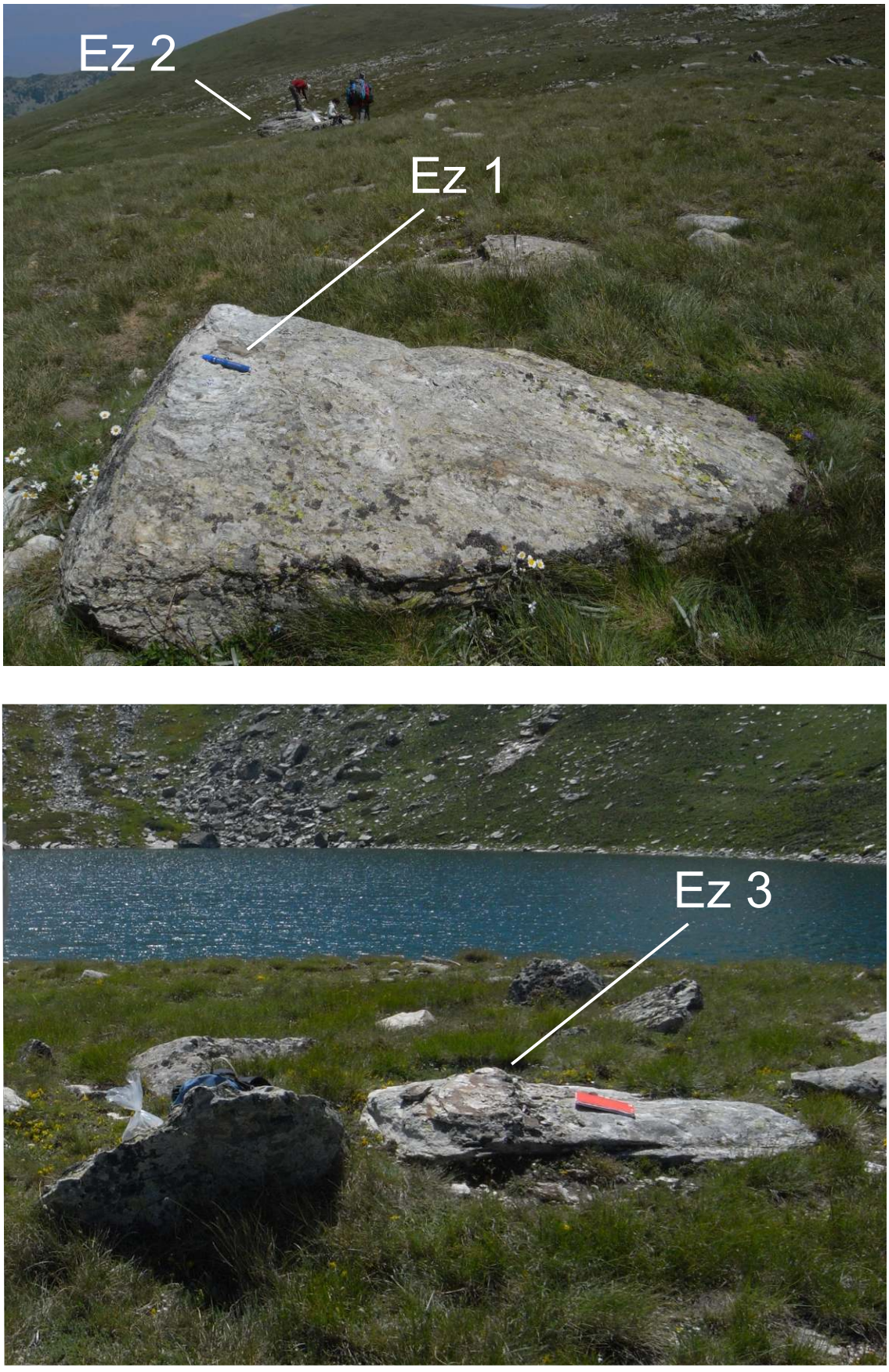

Figure 5

Click here to download Figure FIG_5_LR.pdf

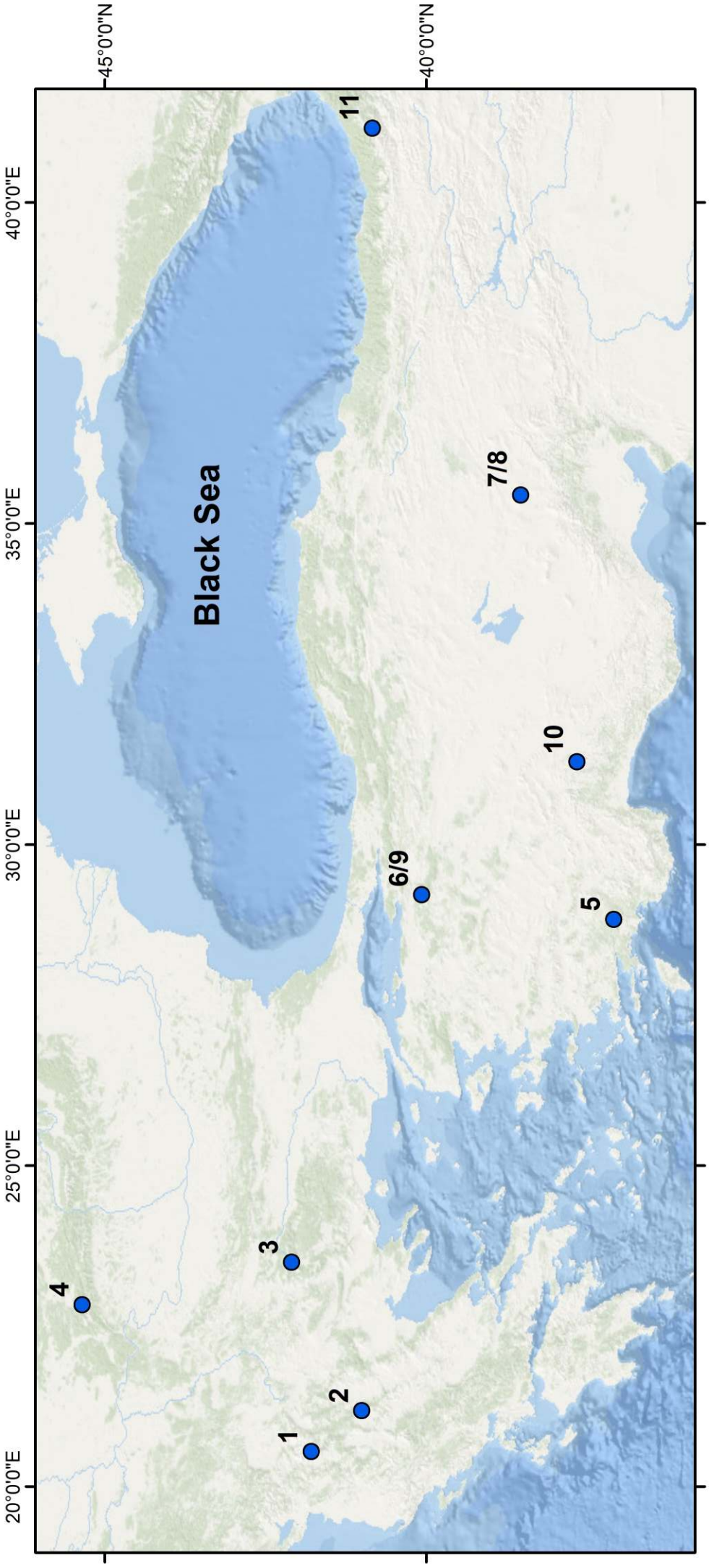

Figure 6

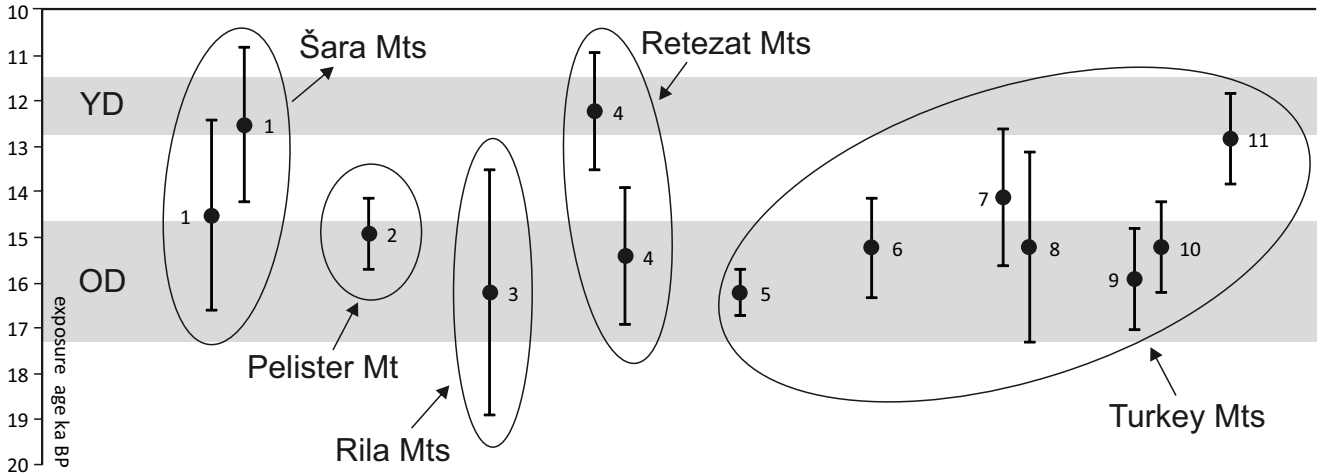

Figure 7

Click here to download Figure FIG_7_LR.pdf

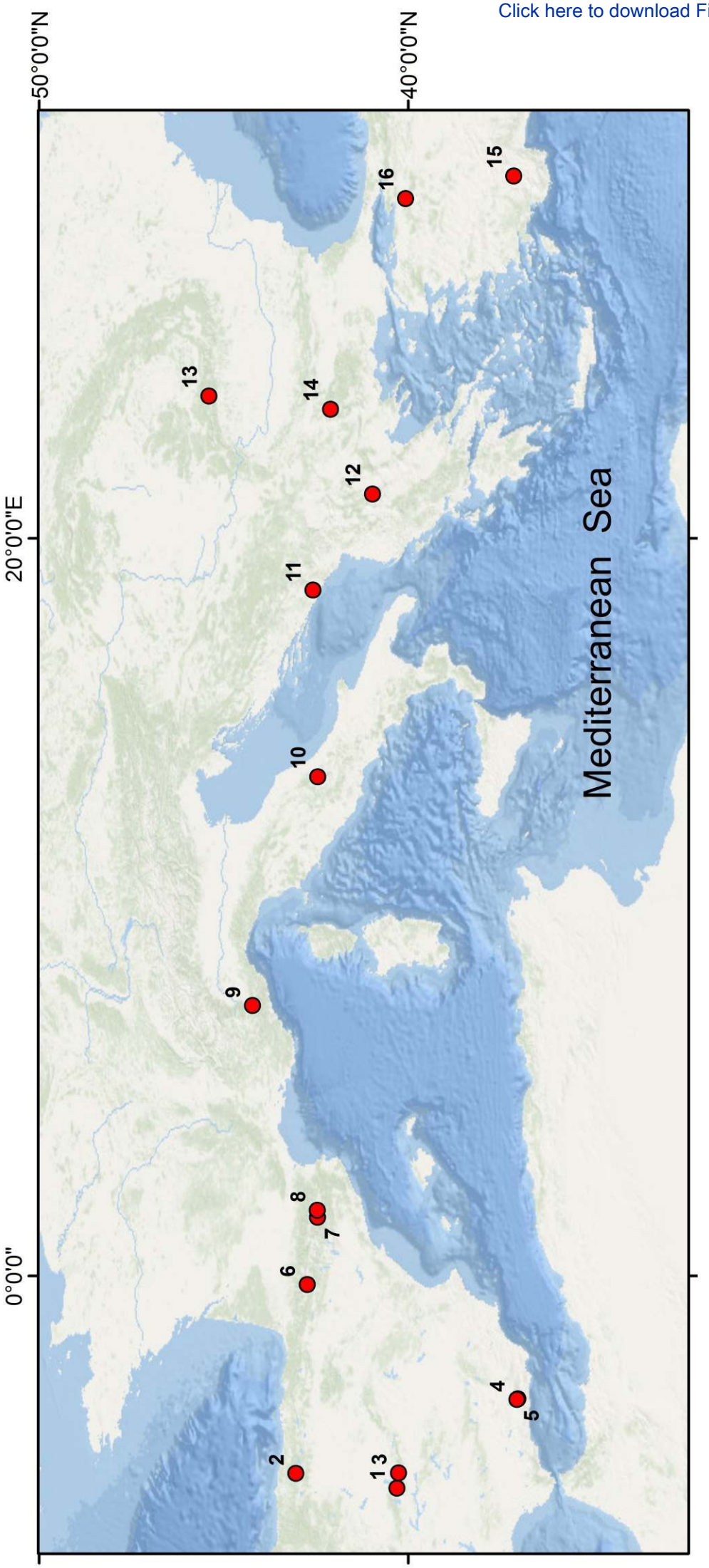

Figure 8

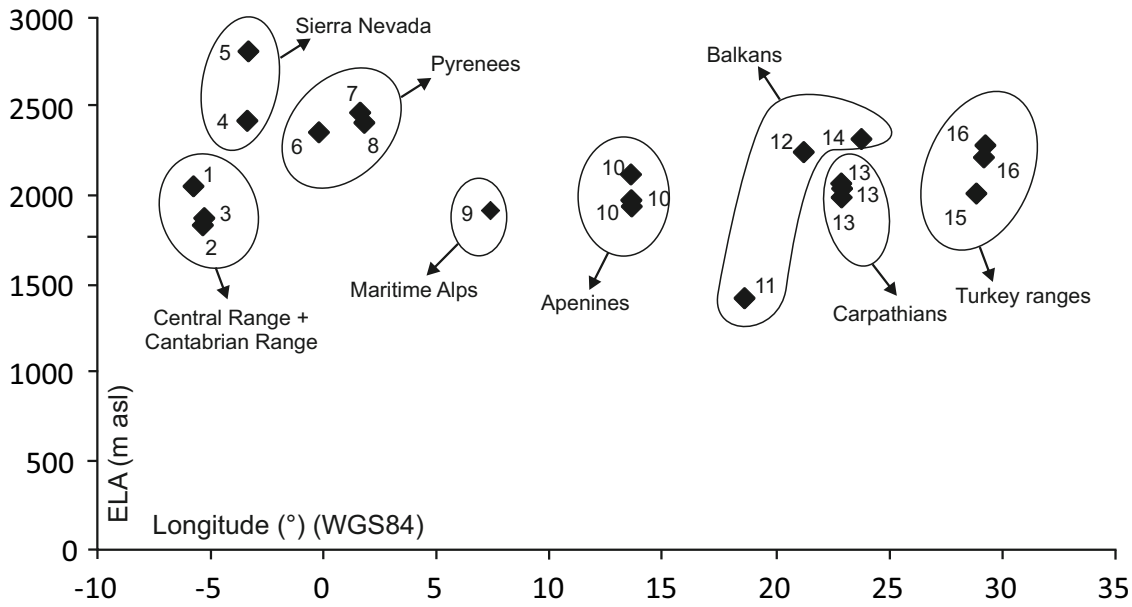

Figure 9